APPROXIMATION OF LARGE BENDING ISOMETRIES WITH DISCRETE KIRCHHOFF TRIANGLES

SÖREN BARTELS

Abstract. We devise and analyze a simple numerical method for the approximation of large bending isometries. The discretization employs a discrete Kirchhoff triangle to deal with second order derivatives and convergence of discrete solutions to minimizers of the continuous formulation is proved. Unconditional stability and convergence of an iterative scheme for the computation of discrete minimizers that is based on a linearization of the isometry constraint is verified. Numerical experiments illustrate the performance of the proposed method.

1. Introduction

A dimension reduction from three-dimensional hyperelasticity with an isotropic energy density with quadratic growth leads to the variational problem of finding a deformation $y:\Omega\to\mathbb{R}^3$ of a bounded Lipschitz domain $\Omega\subset\mathbb{R}^2$ that minimizes the functional

$$E(y)=\frac{\alpha}{2}\int_\Omega |D^2y|^2\,\mathrm{d}x-\int_\Omega f\cdot y\,\mathrm{d}x$$

under the constraint that y is an isometry, i.e., that $(\nabla y)^\top\nabla y=I_2$ almost everywhere in Ω with the identity matrix $I_2\in\mathbb{R}^{2\times 2}$, and subject to the boundary conditions $y=y_{\rm D}$ and $\nabla y=\Phi_{\rm D}$ on $\Gamma_{\rm D}$, e.g., the clamped boundary condition $y(x)=[x,0]^\top$ and $\nabla y(x)=[I_2,0]^\top$ for all $x\in\Gamma_{\rm D}$. Imposing a condition on ∇y on $\Gamma_{\rm D}$ is equivalent to prescribing the normal of the deformed plate along $\Gamma_{\rm D}$. The functional E is the bending energy of the plate described by Ω on which the (rescaled) body force $f\in L^1(\Omega;\mathbb{R}^3)$ is acting. This formulation has recently been rigorously justified in [9] and coincides with the model proposed in [11]. The density results for smooth isometries among isometries in $H^2(\Omega;\mathbb{R}^3)$ proved in [10] allow to replace the Frobenius norm of the second fundamental form of the surface parametrized by y by the Frobenius norm of its Hessian.

In [3] a numerical method for the approximation of minimizers of E has been proposed and analyzed. It is based on the introduction of the additional variable $\Phi\approx\nabla y$ and the penalty term $(t^{-2}/2)\|\Phi-\nabla y\|^2$. This approach allowed to treat the isometry constraint with techniques developed for harmonic maps into surfaces studied in [2]. In this paper we aim at devising a scheme that leads to simpler systems of equations which can be solved effectively. For this we will discretize the Hessian by employing a so-called discrete Kirchhoff triangle. For numerical methods for related nonlinear bending problems we refer the reader to [7, 1, 8, 5].

Finite element methods based on discrete Kirchhoff triangles have been developed in [4] and [12] to approximate linear bending problems. Given a triangulation $\mathcal{T}_h$ of Ω a discrete Kirchhoff triangle defines a linear mapping $\theta_h:W_h\to\Theta_h$ between appropriate finite element spaces W_h and Θ_h that serves as an approximation of the gradient. In the case of the operator constructed in [4] the space $W_h\subset H^1(\Omega)$ consists of continuous functions that are reduced cubic polynomials on each element such that their gradients are continuous at the vertices of elements. The space $\Theta_h\subset H^1(\Omega)$ contains continuous, piecewise quadratic vector fields whose normal derivative is linear along every

Date: November 15, 2011.

1991 *Mathematics Subject Classification.* 65N12, 65N30, 74K20.

Key words and phrases. Discrete Kirchhoff triangles, elasticity, plates, bending energy, isometries.

side of an element. The operator θ_h enables us to define an approximate Hessian by $\nabla\theta_h(w_h)$. The fact that the gradient of a function in W_h is continuous at vertices of elements allows us to impose the isometry constraint at those points. Letting $\mathcal{N}_h$ denote the set of vertices of elements and $\mathcal{I}_h$ the nodal interpolation operator onto the space of continuous, piecewise affine finite elements, we consider the following finite-dimensional constrained minimization problem:

$$\text{(1.1)}\qquad \begin{cases} \text{Minimize } y_h \mapsto E_h(y_h) = \dfrac{\alpha}{2}\displaystyle\int_\Omega |\nabla\theta_h(y_h)|^2\,\mathrm{d}x - \int_\Omega \mathcal{I}_h[f_h\cdot y_h]\,\mathrm{d}x \\ \text{subject to } y_h \in W_h^3 \text{ and } [\nabla y_h(z)]^\top \nabla y_h(z) = I_2 \text{ for all } z\in\mathcal{N}_h, \\ \text{and } y_h(z) = y_{\mathrm{D}}(z),\ \nabla y_h(z) = \Phi_{\mathrm{D}}(z) \text{ for all } z\in\mathcal{N}_h\cap\Gamma_{\mathrm{D}}. \end{cases}$$

For the vector field $y_h \in W_h^3$, the approximate gradient $\theta_h(y_h)$ is obtained by applying θ_h to each component of y_h. We remark that only the nodal values $\big(y_h(z) : z\in\mathcal{N}_h\big)$ and $\big(\nabla y_h(z) : z\in\mathcal{N}_h\big)$ are required for the implementation, in particular, no interpolation of y_h on elements in $\mathcal{T}_h$ is required. We will show that discrete minimizers accumulate at minimizing isometries in $H^2(\Omega;\mathbb{R}^3)$ for the energy functional E.

Our iterative scheme for the practical solution of (1.1) realizes a discrete H^2 gradient flow of the energy functional with a linearization of the nodal isometry constraint about the current iterate. For this it is important to realize that for the employed finite element space W_h the nodal values of the discrete deformation $\big(y_h(z) : z\in\mathcal{N}_h\big)$ and its gradient $\big(\nabla y_h(z) : z\in\mathcal{N}_h\big)$ are independent variables in the minimization problem (1.1). Given an approximation $y_h^n \in W_h^3$ we define

$$\begin{aligned} F_h[y_h^n] = \big\{ w_h \in W_h^3 : {} & [\nabla w_h(z)]^\top \nabla y_h^n(z) + [\nabla y_h^n(z)]^\top \nabla w_h(z) = 0 \text{ for all } z\in\mathcal{N}_h \\ & \text{and } w_h(z) = 0,\ \nabla w_h(z) = 0 \text{ for all } z\in\mathcal{N}_h\cap\Gamma_{\mathrm{D}} \big\} \end{aligned}$$

and compute for $\tau>0$ the correction $d_t y_h^{n+1} \in F_h[y_h^n]$ as the solution of

$$\text{(1.2)}\qquad \big(\nabla\theta_h(d_t y_h^{n+1}), \nabla\theta_h(z_h)\big) + \alpha\big(\nabla\theta_h(y_h^n + \tau d_t y_h^{n+1}), \nabla\theta_h(z_h)\big) = \big(f_h, z_h\big)_h$$

for all $z_h \in F_h[y_h^n]$. The new iterate is defined by $y_h^{n+1} = y_h^n + \tau d_t y_h^{n+1}$. In (1.2), $(\cdot,\cdot)$ denotes the L^2 inner product on Ω with corresponding norm $\|\cdot\|$ and $(\cdot,\cdot)_h$ is defined by $(v,w)_h = \int_\Omega \mathcal{I}_h[vw]\,\mathrm{d}x$. We will show that this iteration is unconditionally stable and energy decreasing in the sense that for all $n\geq 0$ we have

$$\text{(1.3)}\qquad E_h(y_h^{n+1}) + \frac{\tau}{2}\|\nabla\theta_h(d_t y_h^{n+1})\|^2 \leq E_h(y_h^n).$$

The iterates (y_h^n) will in general not satisfy the nodal isometry constraint but provided that the initial deformation y_h^0 satisfies $\big[\nabla y_h^0(z)\big]^\top \nabla y_h^0(z) = I_2$ for all $z\in\mathcal{N}_h$ we have that

$$\text{(1.4)}\qquad \|[\nabla y_h^n]^\top \nabla y_h^n - I_2\|_{L^1_h(\Omega)} \leq C\tau E_h(y_h^0),$$

where $\|v\|_{L^1_h(\Omega)} = \|\mathcal{I}_h v\|_{L^1(\Omega)}$ for a piecewise polynomial function that is continuous in $\mathcal{N}_h$. We remark that the iterates of our scheme satisfy $|\partial_j y_h^n(z)|\geq 1$ for $j=1,2$, $z\in\mathcal{N}_h$, and $n\geq 1$ so that a correction to guarantee $|\partial_j y_h^n(z)| = 1$ can easily be incorporated. Moreover, the scheme can be embedded into multilevel methods owing to its nodal character.

The outline of this article is as follows. In Section 2 we collect some elementary results needed for the definition and analysis of our approximation scheme. Convergence proofs for the discretization in the spirit of variational convergence and for the iterative scheme in terms of a discrete energy law is given in Section 3. In Section 4 some illustrative computational experiments are reported.

2. Preliminaries

2.1. **Finite element spaces.** For a regular triangulation $\mathcal{T}_h$ of Ω into triangles of maximal diameter $h > 0$ we let $\mathcal{N}_h$ denote the set of vertices of elements and $\mathcal{E}_h$ the set of edges of elements. We let $\mathcal{S}^1(\mathcal{T}_h)$ be the space of piecewise affine, globally continuous functions in $H^1(\Omega)$ and $(\varphi_z)_{z\in\mathcal{N}_h}$ the nodal basis of $\mathcal{S}^1(\mathcal{T}_h)$ defined by $\varphi_z(y) = \delta_{zy}$ for all $z, y \in \mathcal{N}_h$. The nodal interpolation operator

$$\mathcal{I}_h v = \sum_{z\in\mathcal{N}_h} v(z)\varphi_z$$

is defined for every function $v \in L^1(\Omega)$ that is continuous at the nodes $z \in \mathcal{N}_h$. We note that for every $1 \le p < \infty$ we have the equivalence

$$c^{-1}\|v_h\|_{L^p(\Omega)}^p \le \sum_{z\in\mathcal{N}_h} \beta_z |v_h(z)|^p \le c\|v_h\|_{L^p(\Omega)}^p \tag{2.1}$$

for all $v_h \in \mathcal{S}^1(\mathcal{T}_h)$ with $\beta_z = \int_\Omega \varphi_z \,\mathrm{d}x$. For an integer $k \ge 0$ we let $\mathcal{P}_k(T)$ be the set of polynomials of degree at most k on $T \in \mathcal{T}_h$ and, if $z_1, z_2, z_3 \in \mathcal{N}_h \cap T$ are the vertices of T and $x_T = (z_1+z_2+z_3)/3$,

$$\mathcal{P}_{3,\mathrm{red}}(T) = \big\{p \in \mathcal{P}_3(T) : 6p(x_T) = \sum_{j=1}^3 \big[2p(z_j) - \nabla p(z_j)\cdot(z_j - x_T)\big]\big\},$$

where the constraint excludes the element bubble function $b_T = \varphi_{z_1}\varphi_{z_2}\varphi_{z_3}$. We then define

$$W_h = \big\{w_h \in C(\overline{\Omega}) : w_h|_T \in \mathcal{P}_{3,\mathrm{red}}(T) \text{ for all } T \in \mathcal{T}_h \text{ and } \nabla w_h \text{ is continuous in } \mathcal{N}_h\big\}$$

and

$$\Theta_h = \big\{\theta_h \in C(\overline{\Omega};\mathbb{R}^2) : \theta_h|_T \in \mathcal{P}_2(T)^2 \text{ and } \theta_h\cdot n_E|_E \text{ is linear for all } E \in \mathcal{E}_h\big\}.$$

Here, $n_E \in \mathbb{R}^2$ is a unit vector that is perpendicular to the edge $E \in \mathcal{E}_h$.

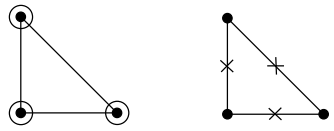

FIGURE 1. Schematic description of the finite element spaces W_h (left) and Θ_h (right).

2.2. **Discrete gradient operator.** The discrete gradient operator $\theta_h : W_h \to \Theta_h$ is for $w_h \in W_h$ defined by the conditions that for $\psi_h = \theta_h(w_h) \in \Theta_h$ we have

$$\psi_h(z) = \nabla w_h(z), \quad \psi_h(z_E)\cdot t_E = \nabla w_h(z_E)\cdot t_E$$

for all $z \in \mathcal{N}_h$ and $E \in \mathcal{E}_h$, where t_E is a unit tangent vector on E and z_E the midpoint of E for every $E \in \mathcal{E}_h$. Owing to the definition of Θ_h we have that $\psi_h(z_E)\cdot n_E = (1/2)\big(\psi_h(z_1)+\psi_h(z_2)\big)\cdot n_E$ for every $E \in \mathcal{E}_h$ with endpoints $z_1, z_2 \in E \cap \mathcal{N}_h$. This implies that

$$\psi_h(z_E) = (1/2)\big[\big(\nabla w_h(z_1) + \nabla w_h(z_2)\big)\cdot n_E\big]n_E + \big[\nabla w_h(z_E)\cdot t_E\big]t_E$$

for every $E \in \mathcal{E}_h$. The mapping θ_h can naturally be extended to functions in $H^3(\Omega) \subset C^1(\overline{\Omega})$.

Lemma 2.1 (Properties of θ_h, [4, 6])**.** *(i) There exist $c_1, c_2 > 0$ such that for all $w_h \in W_h$ and $T \in \mathcal{T}_h$ we have for $\ell = 0, 1$ that*

$$c_1^{-1}\|D^{\ell+1}w_h\|_{L^2(T)} \le \|D^\ell\theta_h(w_h)\|_{L^2(T)} \le c_1\|D^{\ell+1}w_h\|_{L^2(T)},$$

and with $h_T = \mathrm{diam}(T)$

$$\|\theta_h(w_h) - \nabla w_h\|_{L^2(T)} \le c_2 h_T \|D^2 w_h\|_{L^2(T)}.$$

(ii) There exists $c_3 > 0$ such that for all $w \in H^3(\Omega)$ and $T \in \mathcal{T}_h$ we have

$$\|\theta_h(w) - \nabla w\|_{L^2(T)} + h_T \|\nabla \theta_h(w) - D^2 w\|_{L^2(T)} \leq c_3 h_T^2 \|w\|_{H^3(T)}.$$

(iii) The mapping $w_h \mapsto \|\nabla \theta_h(w_h)\|$ defines a norm on $\{w_h \in W_h : w_h(z) = 0,\ \nabla w_h(z) = 0$ for all $z \in \mathcal{N}_h \cap \Gamma_{\mathrm{D}}\}$.

Proof. The estimates follow from linearity of the mapping $w_h \mapsto \theta_h(w_h)$, injectivity of $\nabla w_h \mapsto \theta_h(w_h)$, the Bramble-Hilbert lemma, and transformation arguments, cf. [4, 6] for details. □

3. Approximation and computation

We assume in the following that $y_{\mathrm{D}} \in C(\Gamma_{\mathrm{D}}; \mathbb{R}^3)$ and $\Phi_{\mathrm{D}} \in C(\Gamma_{\mathrm{D}}; \mathbb{R}^{3\times 2})$ are compatible in the sense that there exists an isometry $\widetilde{y}_{\mathrm{D}} \in H^2(\Omega; \mathbb{R}^3)$ with $\widetilde{y}_{\mathrm{D}}|_{\Gamma_{\mathrm{D}}} = y_{\mathrm{D}}$, $\nabla \widetilde{y}_{\mathrm{D}}|_{\Gamma_{\mathrm{D}}} = \Phi_{\mathrm{D}}$ on Γ_{D}, and that every such isometry can be approximated in $H^2(\Omega; \mathbb{R}^3)$ by smooth isometries with the same boundary conditions, cf. [10]. We suppose that y_{D} and Φ_{D} can be approximated with arbitrary accuracy by nodal interpolation on Γ_{D}, i.e., we have for $h \to 0$ that

$$\big\|y_{\mathrm{D}} - \mathcal{I}_h \widetilde{y}_{\mathrm{D}}|_{\Gamma_{\mathrm{D}}}\big\|_{L^2(\Gamma_{\mathrm{D}})} + \big\|\Phi_{\mathrm{D}} - \mathcal{I}_h \nabla \widetilde{y}_{\mathrm{D}}|_{\Gamma_{\mathrm{D}}}\big\|_{L^2(\Gamma_{\mathrm{D}})} \to 0.$$

Theorem 3.1 (Approximation)**.** *Let $(\mathcal{T}_h)_{h>0}$ be a sequence of triangulations of Ω and assume that $f_h \in \mathcal{S}^1(\mathcal{T}_h)$ satisfies $f_h \rightharpoonup f$ in $L^2(\Omega; \mathbb{R}^3)$ as $h \to 0$. For each $h > 0$ there exists a minimizer $y_h \in W_h^3$ for (1.1) and if $(y_h)_{h>0}$ is a sequence of (almost) minimizers then $\|\nabla y_h\| \leq C$ for all $h > 0$ and every accumulation point $y \in H^1(\Omega; \mathbb{R}^3)$ of the sequence is a strong accumulation point, belongs to $H^2(\Omega; \mathbb{R}^3)$, satisfies $(\nabla y)^\top \nabla y = I_2$ almost everywhere in Ω, $y|_{\Gamma_{\mathrm{D}}} = y_{\mathrm{D}}$, and $\nabla y|_{\Gamma_{\mathrm{D}}} = \Phi_{\mathrm{D}}$, and is a minimizer of E.*

Proof. By Lemma 2.1 (iii) we have that $\|\nabla \theta_h(y_h)\|$ is a norm and this implies that (1.1) has a solution. Owing to the assumptions on the boundary data it follows with Poincaré's inequality and Lemma 2.1 (i) that that $\|\nabla y_h\| \leq C$ and $\|\nabla \theta_h(y_h)\| \leq C$ for all $h > 0$. Let $y \in H^1(\Omega; \mathbb{R}^3)$ and $z \in H^1(\Omega; \mathbb{R}^{3\times 2})$ be such that for a subsequence (which is not relabeled) we have $y_h \rightharpoonup y$ in $H^1(\Omega; \mathbb{R}^3)$ and $\theta_h(y_h) \rightharpoonup z$ in $H^1(\Omega; \mathbb{R}^{3\times 2})$. With Lemma 2.1 we verify that $\|\theta_h(y_h) - \nabla y_h\| \leq ch\|\nabla \theta_h(y_h)\|$ and this yields $\nabla y = z$, in particular $y \in H^2(\Omega; \mathbb{R}^3)$. The attainment of the boundary conditions follows from continuity of the trace operators and the fact that $\|y_h - \mathcal{I}_h y_h\| + \|\theta_h(y_h) - \mathcal{I}_h \theta_h(y_h)\| \to 0$ as $h \to 0$. A nodal interpolation estimate and an inverse inequality yield that

$$\big\|\big(\nabla y_h\big)^\top \nabla y_h - I_2\big\|_{L^1(T)} \leq ch\|D^2 y_h\|_{L^2(T)} \|\nabla y_h\|_{L^2(T)}$$

and this implies after summation over all $T \in \mathcal{T}_h$ together with fact that ∇y_h converges strongly to ∇y that $(\nabla y)^\top \nabla y = I_2$ almost everywhere in Ω. To verify that y minimizes E we first notice that by weak lower semicontinuity of the L^2 norm we have

$$\|D^2 y\| = \|\nabla z\| \leq \liminf_{h\to 0} \|\nabla \theta_h(y_h)\|$$

and

$$\int_\Omega \mathcal{I}_h[y_h \cdot f_h]\,\mathrm{d}x = \int_\Omega y_h \cdot f_h\,\mathrm{d}x + \int_\Omega \big\{y_h \cdot f_h - \mathcal{I}_h[y_h \cdot f_h]\big\}\,\mathrm{d}x,$$

where the first term converges to $\int_\Omega y \cdot f\,\mathrm{d}x$ whereas the second one converges to zero owing to standard interpolation results and inverse estimates. This implies that

$$E(y) \leq \liminf_{h\to 0} E_h(y_h).$$

To show that the minimal energy is attained let $\widetilde{y} \in H^2(\Omega; \mathbb{R}^3)$ be a minimizing isometry for E. Owing to the density results from [10] we may assume that $\widetilde{y} \in C^\infty(\Omega; \mathbb{R}^3)$. We then let $\widetilde{y}_h \in W_h^3$

be the interpolant of $\widetilde{y}$ (the uniquely defined function $\widetilde{y}_h \in W_h^3$ that satisfies $\widetilde{y}_h(z) = \widetilde{y}(z)$ and $\nabla\widetilde{y}_h(z) = \nabla\widetilde{y}(z)$ for all $z \in \mathcal{N}_h$). We then have with Lemma 2.1 (ii) that

$$\|\theta_h(\widetilde{y}_h) - \nabla\widetilde{y}\| + h\|\nabla\theta_h(\widetilde{y}_h) - D^2\widetilde{y}\| \le ch^2\|\widetilde{y}\|_{H^3(\Omega)}$$

which implies the attainment of the minimal energy. This concludes the proof of the theorem. □

Theorem 3.2 (Computation)**.** *Given $\tau > 0$ and $y_h^0 \in W_h^3$ such that $y_h^0(z) = y_{\mathrm{D}}(z)$ and $\nabla y_h^0(z) = \Phi_{\mathrm{D}}(z)$ for all $z \in \mathcal{N}_h \cap \Gamma_{\mathrm{D}}$ and $[\nabla y_h^0(z)]^\top \nabla y_h^0(z) = I_2$ for all $z \in \mathcal{N}_h$ there exists for each $n \ge 0$ a unique function $d_t y_h^{n+1} \in F_h[y_h^n]$ that satisfies* (1.2)*. For the sequence $(y_h^n)_{n\ge 0}$ inductively defined by $y_h^{n+1} = y_h^n + \tau d_t y_h^{n+1}$ we have* (1.3) *and* (1.4)*.*

Proof. The existence of a unique $d_t y_h^{n+1} \in F_h[y_h^n]$ that solves (1.2) follows from the fact that the bilinear form $(v_h, w_h) \mapsto \big(\nabla\theta_h(v_h), \nabla\theta_h(w_h)\big)$ defines a coercive continuous bilinear form on $F_h[y_h^n]$, cf. Lemma 2.1 (iii). Upon choosing $z_h = d_t y_h^{n+1}$ we find that

$$\big\|\nabla\theta_h(d_t y_h^{n+1})\big\|^2 + \frac{\alpha}{2} d_t \big\|\nabla\theta_h(y_h^{n+1})\big\|^2 + \frac{\alpha\tau}{2}\big\|\nabla\theta_h(d_t y_h^{n+1})\big\|^2 = \big(f_h, d_t y_h^{n+1}\big)_h$$

and this gives (1.3). Using $y_h^{n+1} = y_h^n + \tau d_t y_h^{n+1}$ we have

$$\big(\nabla y_h^{n+1}\big)^\top \nabla y_h^{n+1} = \big(\nabla y_h^n\big)^\top \nabla y_h^n + \tau\big(\nabla d_t y_h^{n+1}\big)^\top \nabla y_h^n + \tau\big(\nabla y_h^n\big)^\top \nabla d_t y_h^{n+1} + \tau^2\big(\nabla d_t y_h^{n+1}\big)^\top \nabla d_t y_h^{n+1}.$$

Since $d_t y_h^{n+1} \in F_h[y_h^n]$ the sum of the second and third term on the right-hand side vanishes at every $z \in \mathcal{N}_h$ and an inductive argument leads to

$$\big|\big[\nabla y_h^{n+1}(z)\big]^\top \nabla y_h^{n+1}(z) - I_2\big| \le \tau^2 \sum_{\ell=0}^{n} \big|\nabla d_t y_h^{\ell+1}(z)\big|^2.$$

The norm characterization (2.1), nodal interpolation estimates, and a local inverse inequality imply the assertion. □

4. Numerical experiments

To illustrate the practical performance of our scheme and our algorithm we study two prototypical specifications of the model problem. These are defined by a vertical load with a fixed part of the boundary of the plate and compressive boundary conditions, respectively. In all of our experiments we employed triangulations $\mathcal{T}_h = \mathcal{T}_\ell$ determined by a positive integer ℓ that consist of halved squares with edge-lengths $\widehat{h} = 2^{-\ell}$ and diameters $h = \sqrt{2}\,\widehat{h}$. The time-step size for the iterative scheme was chosen as $\tau = \widehat{h}$ unless otherwise stated and as a stopping criterion for the iteration we used $\|d_t\nabla\theta_h(y_h^{n+1})\| \le \varepsilon_{stop} = 1.0 \times 10^{-3}$. To display the discrete deformations $y_h \in W_h^3$ we always plotted its nodal interpolant $\mathcal{I}_h y_h$. Our finest triangulations consisted of 131.072 triangles and the overall CPU time needed to compute the corresponding discrete solutions defined by 544.441 degrees of freedom was on the order of a few hours on these meshes.

Remarks 4.1. *If S is the stiffness matrix related to piecewise quadratic vector fields with six components, T realizes the operator $\theta_h : W_h^3 \to \Theta_h^3$, and B_n encodes the constraints and boundary conditions defined in the space $F_h[y_h^n]$, then one step of the discrete gradient flow leads to the linear system of equations*

$$\begin{bmatrix} (1+\alpha\tau)T^\top S T & B_n^\top \\ B_n & 0 \end{bmatrix} \begin{bmatrix} d_t Y^{n+1} \\ \Lambda \end{bmatrix} = \begin{bmatrix} -\tau T^\top S T\, Y^n + \tau F \\ 0 \end{bmatrix}$$

In our implementation these linear systems of equations were solved with a direct solver.
(ii) If $w_h|_E$ is cubic we have $\nabla w_h(z_E)\cdot t_E = (3/(2\ell_E))\big(w_h(z_2) - w_h(z_1)\big) - (1/4)\big(\nabla w_h(z_1) + \nabla w_h(z_2)\big)\cdot t_E$ with ℓ_E and $z_1, z_2 \in \mathcal{N}_h \cap E$ such that $z_2 - z_1 = \ell_E t_E$.

For a deformation $y_h \in W_h^3$ we set $\nu_h = \mathcal{I}_h[\partial_1 y_h \times \partial_2 y_h]$ and define the quantities

$$\delta I_h = \left|\left(\nabla[\mathcal{I}_h y_h]\right)^\top \nabla[\mathcal{I}_h y_h] - I_2\right|, \quad K_h = \det\left(\nabla \nu_h\right)^\top \nabla[\mathcal{I}_h y_h],$$

that measure the deviation of a discrete first fundamental form from the identity, i.e., how much y_h fails to be an isometry, and provide an approximation of the Gaussian curvature, respectively.

4.1. **Vertical load on a square-shaped plate.** In the first experiment the plate is square-shaped, clamped along two non-parallel sides, and subject to a vertical load.

Example 4.1. *Let* $\Omega = (0,4) \times (0,4)$, $\Gamma_{\mathrm{D}} = \{0\} \times [0,4] \cup [0,4] \times \{0\}$, $\alpha = 1$, $y_{\mathrm{D}}(x) = (x,0)^\top$ *and* $\Phi_{\mathrm{D}}(x) = [I_2, 0]^\top$ *for all* $x \in \Gamma_{\mathrm{D}}$, *and* $f(x) = c_f(0,0,1)^\top$ *for* $x \in \Omega$ *with* $c_f = 2.5 \times 10^{-2}$.

In Figure 2 we plotted the discrete deformations obtained with our numerical scheme together with the modulus of the approximate Gaussian curvature K_h for the triangulations $\mathcal{T}_3$, $\mathcal{T}_4$, and $\mathcal{T}_5$. Owing to Gauss' *theorema egregium* every exact solution defines a surface with vanishing Gaussian curvature. In the plots of the numerical approximations we see that the discrete Gaussian curvature does not vanish but becomes small as the mesh-size is decreased and that it is largest along the diagonal $\{x + y = 4\}$. Closely related is the observation that the maximal displacement decreases as the mesh-size becomes smaller, i.e., the relaxation of the isometry condition becomes less and less soft. Every exact deformation has to be the identity in the region $\{x \leq 4 - y\}$. The inexact treatment of the isometry condition leads to an artificial displacement in this region. To illustrate the convergence of this error, we plotted in Figure 3 the discrete deformations along the diagonal $\{x + y = 4\}$ and we observe that the maximum decays to zero. In Table 1 we displayed for different triangulations and fixed relation $\tau = \widehat{h}$ the numbers of iterations required to satisfy the stopping criterion, the computed discrete energy, the L^1 norm of the difference between the discrete fundamental form and the identity matrix, and the L^1 norm of the discrete Gaussian curvature. We see that the number of iterations increases by a factor 2 whenever the mesh-size is halved. The approximation of the Gaussian curvature and the error in the discretization of the isometry constraint approach an experimental rate of convergence close to 1. We remark that our results were independent of geometrical properties of the underlying triangulations and that in this experiment smaller time-step sizes and finer stopping criteria did not lead to significant changes in the numerical approximations.

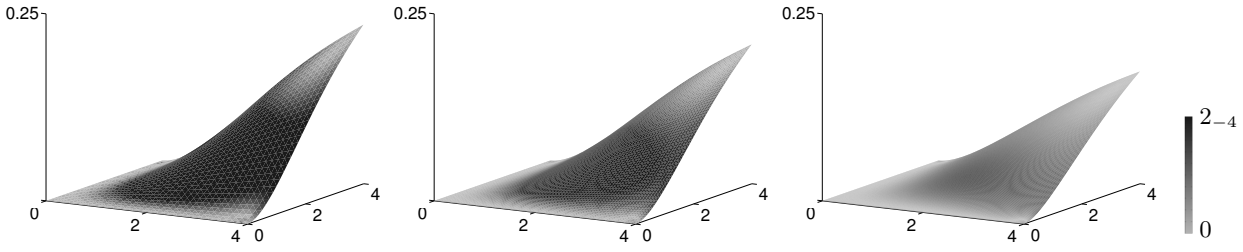

FIGURE 2. Discrete deformations of a clamped 4×4 plate subject to a uniform vertical load and modulus of corresponding discrete Gaussian curvature on the triangulations $\mathcal{T}_3$, $\mathcal{T}_4$, and $\mathcal{T}_5$ in Example 4.1.

4.2. **Compression of a strip.** We next study compressive boundary conditions on a part of the boundary of a rectangular plate. A small vertical load selects one of at least two possible solutions related to the symmetry in vertical direction of the problem for $f = 0$.

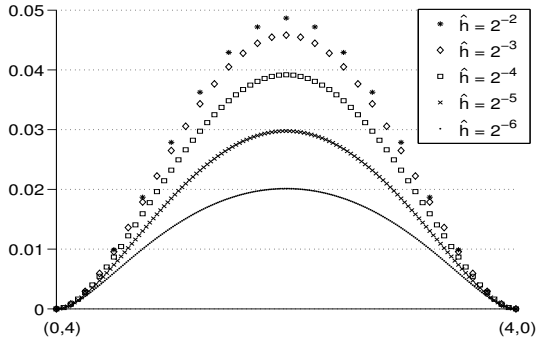

FIGURE 3. Artificial discrete displacements along the diagonal $\{(x, y) \in \Omega : x+y = 4\}$ for different mesh-sizes in Example 4.1.

$\widehat{h}$	N_{iter}	$E_h(y_h)$	$\|\delta I_h\|_{L^1(\Omega)}$	$\|K_h\|_{L^1(\Omega)}$
2^{-2}	22	-1.009_{-2}	8.674_{-3}	3.389_{-3}
2^{-3}	40	-9.821_{-3}	7.124_{-3}	3.043_{-3}
2^{-4}	71	-9.041_{-3}	5.143_{-3}	2.308_{-3}
2^{-5}	130	-7.666_{-3}	3.032_{-3}	1.469_{-3}
2^{-6}	272	-6.024_{-3}	1.511_{-3}	8.656_{-4}

TABLE 1. Iteration numbers, computed energy, deviation of the discrete first fundamental form from I_2, and L^1 norm of the discrete Gaussian curvature for different mesh-sizes and time-step size $\tau = \widehat{h}$ in Example 4.1.

Example 4.2. *Let* $\Omega = (-2, 2) \times (0, 1)$, $\Gamma_{\mathrm{D}} = \{-2, 2\} \times [0, 1]$, $\alpha = 1$, $f(x) = c_f(0, 0, 1)^\top$ *with* $c_f = 1.0 \times 10^{-5}$ *for* $x \in \Omega$, $\Phi_{\mathrm{D}} = [I_2, 0]^\top$ *on* Γ_{D}, *and*

$$y_{\mathrm{D}}(x) = (x_1 \pm a, x_2, 0)^\top$$

for $(x_1, x_2) \in \Gamma_{\mathrm{D}}$ *with* $x_1 = \mp 2$. *We set* $a = 1.4$.

For the triangulation $\mathcal{T}_5$ we ran our iterative scheme with $\tau = \widehat{h}^\beta$ for $\beta = 0.5, 1.0, 1.5$. The computed deformations together with the quantity δI_h are shown in the plots of Figure 4. The symmetry of the problem implies a non-trivial displacement only in one coordinate direction so that the approximation error of the exact Gaussian curvature is very small in this experiment. A strong violation of the isometry constraint is however observable in large regions of the deformed plate for the large time-step size defined through $\beta = 0.5$. The results for the time-step sizes specified through the exponents $\beta = 1.0$ and $\beta = 1.5$ lead to a smaller error δI_h and the corresponding computed deformations differ significantly. Similar conclusions can be drawn for the numbers displayed in Table 2. The L^1 norm of δI_h for $\beta = 1.5$ is notably smaller than for the larger time-step sizes. The expense for the more accurate approximation of the isometry constraint is a larger number of iterations. The iteration numbers in this experiment increased by a factor approximately 5 whenever we increased the exponent β by 0.5. We remark that we employed a simple extension of the boundary data to initialize the iteration.

REFERENCES

[1] BARRETT, J. W., GARCKE, H., AND NÜRNBERG, R. On the variational approximation of combined second and fourth order geometric evolution equations. *SIAM J. Sci. Comput. 29*, 3 (2007), 1006–1041 (electronic).

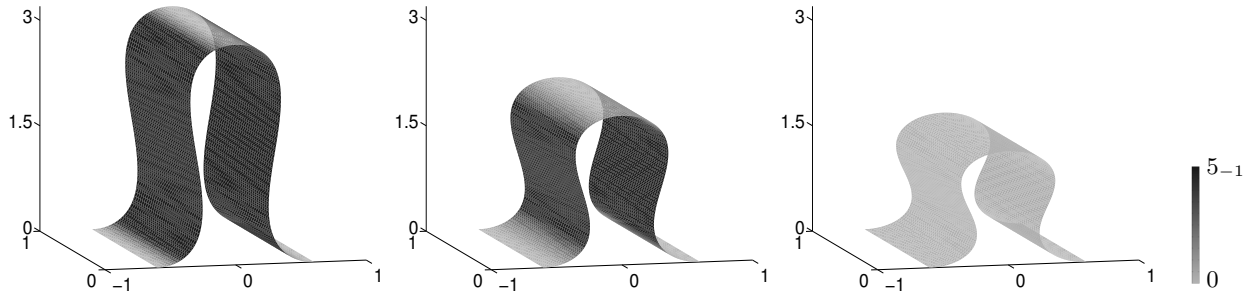

FIGURE 4. Discrete deformations for the compression of a 4×1 plate with a small uniform vertical load on the triangulation $\mathcal{T}_5$ obtained with the time-step size $\tau = \widehat{h}^\beta$ for $\beta = 0.5$, 1.0, 1.5. The deformations are colored by the error δI_h.

τ	N_{iter}	$E_h(y_h)$	$\|\delta I_h\|_{L^1(\Omega)}$	$\|K_h\|_{L^1(\Omega)}$
$\widehat{h}^{0.5}$	84	1.843_{+1}	$8.643_{\pm 0}$	9.256_{-9}
$\widehat{h}^{1.0}$	440	1.095_{+1}	$2.269_{\pm 0}$	1.826_{-9}
$\widehat{h}^{1.5}$	2.457	$8.638_{\pm 0}$	6.913_{-2}	1.431_{-9}

TABLE 2. Iteration numbers, computed energy, deviation of the discrete first fundamental form from I_2, and L^1 norm of the discrete Gaussian curvature for the mesh-size $\widehat{h} = 2^{-5}$ and time-step sizes $\tau = \widehat{h}^\beta$ for $\beta = 0.5$, 1.0, 1.5 in Example 4.2.

[2] BARTELS, S. Numerical analysis of a finite element scheme for the approximation of harmonic maps into surfaces. *Math. Comp. 79*, 271 (2010), 1263–1301.

[3] BARTELS, S. Finite element approximation of large bending isometries. Preprint, 2011.

[4] BATOZ, J.-L., BATHE, K.-J., AND HO, L.-W. A study of three-node triangular plate bending elements. *International Journal for Numerical Methods in Engineering 15*, 12 (1980), 1771–1812.

[5] BONITO, A., NOCHETTO, R. H., AND PAULETTI, M. S. Parametric FEM for geometric biomembranes. *J. Comput. Phys. 229*, 9 (2010), 3171–3188.

[6] BRAESS, D. *Finite elements*. Cambridge University Press, Cambridge, 2007.

[7] DU, Q., LIU, C., RYHAM, R., AND WANG, X. A phase field formulation of the Willmore problem. *Nonlinearity 18*, 3 (2005), 1249–1267.

[8] DZIUK, G. Computational parametric Willmore flow. *Numer. Math. 111*, 1 (2008), 55–80.

[9] FRIESECKE, G., JAMES, R. D., AND MÜLLER, S. A theorem on geometric rigidity and the derivation of nonlinear plate theory from three-dimensional elasticity. *Comm. Pure Appl. Math. 55*, 11 (2002), 1461–1506.

[10] HORNUNG, P. Approximating $W^{2,2}$ isometric immersions. *C. R. Math. Acad. Sci. Paris 346*, 3-4 (2008), 189–192.

[11] KIRCHHOFF, G. R. Über das Gleichgewicht und die Bewegung einer elastischen Scheibe. *J. Reine Angew. Math. 40* (1850), 51–88.

[12] ZIENKIEWICZ, O. *The Finite Element Method in Structural and Continuum Mechanics*. McGraw-Hill, London, 1971.

INSTITUTE FOR NUMERICAL SIMULATION, RHEINISCHE FRIEDRICH-WILHELMS-UNIVERSITÄT BONN, WEGELERSTR. 6, 53115 BONN, GERMANY

E-mail address: bartels@ins.uni-bonn.de